Since January 2020 Elsevier has created a COVID-19 resource centre with free information in English and Mandarin on the novel coronavirus COVID-19. The COVID-19 resource centre is hosted on Elsevier Connect, the company's public news and information website.

VIROLOGY 187, 627–632 (1992)

Rabies Virus Glycoprotein Is a Trimer

YVES GAUDIN,*,[1] ROB W. H. RUIGROK,† CHRISTINE TUFFEREAU,* MARCEL KNOSSOW,‡ AND ANNE FLAMAND*

*Laboratoire de génétique des virus, CNRS, 91198 Gif sur Yvette cédex, France; †EMBL Grenoble Outstation c/o ILL, 156X, 38042 Grenoble cédex, France; and ‡Laboratoire de biologie physico-chimique (CNRS URA 1132), bat. 433, Université de Paris Sud, 91405 Orsay cédex, France

Received November 15, 1991; accepted January 8, 1992

The oligomerization state of the rabies virus envelope glycoprotein (G protein) was determined using electron microscopy and sedimentation analysis of detergent solubilized G. Most of the detergents used in this study solubilized G in a 4 S monomeric form. However, when CHAPS was used, G had a sedimentation coefficient of 9 S. This high sedimentation coefficient allowed its further separation from M1 and M2. Using electron microscopy of negatively stained samples, we studied the morphology of G on virus and after detergent extraction. End-on views of G on virus clearly showed triangles consisting of three dots indicating the trimeric nature of native G. End-on views of CHAPS-isolated G showed very similar triangles confirming that, using this detergent, G was solubilized in its native trimeric structure. Electron microscopy also showed that G had a "head" and a "stalk" and provided the basis for a low-resolution model of the glycoprotein structure.

The glycoprotein (G) of rabies virus is the only surface protein of the virion. It constitutes the spikes which protrude from the viral surface and plays a critical role in virus infection. First, it initiates the interaction between the virus and the target cell: it is responsible for virus attachment to specific receptors on the cell (Wunner *et al.*, 1984) and, therefore, is important in determining the tissue tropism of the virus (Kucera *et al.*, 1985; Coulon *et al.*, 1989; Lafay *et al.*, 1991). Second, after attachment to the host cell and internalization of the virion via the endocytic pathway, the G protein mediates the low pH-induced fusion of the viral envelope with the endocytic vesicle membrane (Mifune *et al.*, 1982; Gaudin *et al.*, 1991a). Finally, the G protein stimulates the host immune system and induces the synthesis of neutralizing antibodies (Wiktor *et al.*, 1973).

The complete glycoprotein molecule is 505 amino acids long (Anilionis *et al.*, 1981; Yelverton *et al.*, 1983). Its predicted amino acid sequence indicates that it has three potential N-linked oligosaccharide acceptor sites, of which only one or two are glycosylated (Dietzschold, 1977; Dietzschold *et al.*, 1979; Wunner *et al.*, 1985). Polyacrylamide gel electrophoresis shows that for the CVS and PM strains of rabies virus two forms of G exist (Arita and Atanasiu, 1980) which have, respectively, one and two carbohydrate chains (Dietzschold *et al.*, 1979; Wunner *et al.*, 1985). The glycoprotein is also palmitoylated on a cysteine situated on the C-terminal side of its transmembrane region (Gaudin *et al.*, 1991b). The entity which constitutes a spike at the viral surface has been reported to be an oligomer of G (Dietzschold *et al.*, 1978; Delagneau *et al.*, 1981), but whether it was a trimer as it has been suggested for the glycoprotein of vesicular stomatitis virus (VSV) (Doms *et al.*, 1987) was not established.

In this paper, using high electron microscopy of negatively stained samples and hydrodynamic techniques, we have studied the oligomeric structure of G both on the viral surface and after solubilization with detergents. These studies clearly show that the native quaternary structure of G is trimeric. However, most detergents used in this study solubilized G in a monomeric form and only CHAPS, a zwitterionic detergent, allowed solubilization of G in its native trimeric structure. Our results also provide the basis for a low-resolution model of the glycoprotein structure.

MATERIALS AND METHODS

Chemicals

Octyl glucoside (OG) and decanoyl-*N*-methyl glucamide (MEGA 10) were purchased from Boehringer. 3-[(3-cholamidopropyl)dimethyl-ammonio]-1-propane sulfonate (CHAPS) was bought from Sigma Chemical Co, 6-*O*-(*N*-heptylcarbamoyl)-methyl-α-D-glucopyranoside (Hecameg) was from Vegatec (France), and Triton X-100 was from Prolabo (France).

Cells

BSR cells, a clone of BHK 21 (baby hamster kidney), were grown in Eagle's minimal essential medium (MEM) supplemented with 10% calf serum.

[1] To whom reprint requests should be addressed.

0042-6822/92 $3.00

Viruses

The CVS strain of rabies virus and the antigenic mutant 50L1, mutated at amino acid 333 of the viral glycoprotein (Arg to Glu), were grown in BSR cells at 37° in MEM supplemented with 2% calf serum. Virus particles were pelleted from the culture fluid 72 hr postinfection through 30% glycerol in 10 m*M* Tris–HCl, pH 7.5, 50 m*M* NaCl, 1 m*M* EDTA, and resuspended in TD (137 m*M* NaCl, 5 m*M* KCl, 0.7 m*M* Na_2HPO_4, 25 m*M* Tris–HCl, pH 7.5, 10 m*M* EDTA).

Solubilization and purification of G protein

One volume of virus in TD (4 mg/ml) was added to 1 vol of solubilization buffer (TD plus 2 μg/ml leupeptin, 2 μg/ml antipain, 2 μg/ml pepstatin, 2 μg/ml chymostatin, 16 μg/ml aprotinin) containing 2% CHAPS. The mixture was incubated for 30 min at 37° and then overlayed on 20% sucrose in TD plus 1% CHAPS and centrifuged for 1 hr at 35K to separate solubilized glycoprotein from the rest of the virus particle. The supernatant mainly containing G was then applied onto a 5–20% sucrose gradient in TD plus 1% CHAPS and centrifuged for 16 hr at 35,000 rpm in an SW41 rotor (Beckman). Twelve fractions were collected and analyzed by sodium dodecyl sulfate–polyacrylamide gel electrophoresis (SDS–PAGE). The fractions containing G were concentrated on Centricon 30 (Amicon) and conserved at 4°. The sedimentation coefficient of G was determined on the sucrose gradient using BSA (4.6 S), influenza hemagglutinin (9 S), and catalase (11 S) as sedimentation standards.

SDS–PAGE

Fourteen percent SDS–PAGE of proteins were performed as described by Laemmli (1970). They were stained with Coomassie brilliant blue.

Electron microscopy

Samples were diluted with PBS (150 m*M* NaCl; 10 m*M* phosphate buffer, pH 7.4) or PBS plus 1% CHAPS (see Results) to a protein concentration of 50 μg/ml. A small droplet was applied to the edge of a piece of carbon film on mica upon which the droplet was sucked into the carbon/mica interface and the sample adsorbed onto the clean face of the carbon film. The carbon film plus sample was then floated on a solution of 1% sodium silicotungstate (SST), picked up with an EM grid, and subsequently air-dried. Pictures were taken on a Jeol 100CXII electron microscope at a magnification of 40K under low-dose conditions. The magnification was calibrated using the 17.5-nm spacing of negatively stained catalase crystals. Measurements were made from prints of 160K magnification with a graticule eyepiece giving additional magnification of 8×.

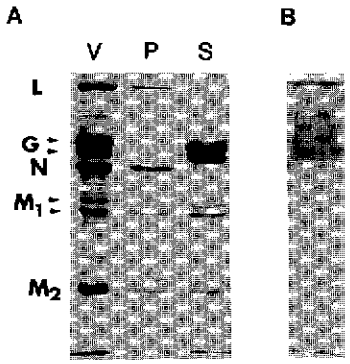

FIG. 1. Purification of G (from 50L1). (A) SDS–PAGE under reducing conditions of: V, virus before treatment with CHAPS; P, viral nucleocapsids pelleted by centrifugation after virus treatment with 1% CHAPS (see Material and Methods); and S, supernatant containing viral proteins solubilized with 1% CHAPS. (B) SDS–PAGE under reducing conditions of the fraction 9S from the sucrose gradient (in TD plus 1% CHAPS) indicating that G was obtained essentially free from contaminants.

RESULTS

Solubilization and purification of the glycoprotein

Several detergents were used, with variable success, to solubilize the glycoprotein from purified virions. For instance, OG (3%) and HECAMEG (1.5%) did not efficiently solubilize the protein: after the first centrifugation (see Material and Methods), G was found in the pellet associated with the nucleocapsids (data not shown). Other detergents (0.7% of MEGA 10, 0.5% of Triton X100, 1% of THESIT) were efficient. However, using these detergents, the solubilized glycoprotein had a sedimentation coefficient of approximately 4S (Fig. 2B) which, by comparison with VSV glycoprotein (Doms *et al.*, 1987) or with BSA, indicated that it was monomeric and therefore had lost its putative quaternary structure. As the trimeric structure of VSV glycoprotein is stabilized at slightly acidic pH (Doms *et al.*, 1987), we also tried to solubilize G with Triton X100 at pH 5.7 as described for VSV. In this case, G was also monomeric.

Finally, we decided to use CHAPS, a zwitterionic detergent, which efficiently solubilized G together with some M1 and M2 (Fig. 1A). In the presence of 1% CHAPS (16.2 m*M*), G had an apparent sedimentation coefficient of 9 S (Fig. 2A) and could be separated from the two other proteins (Fig. 1B). This sedimentation coefficient was very similar to that of native influenza HA (9 S) (Brand and Skehel, 1972) and VSV glycoprotein (8 S) (Doms *et al.*, 1987), both of which are trimeric. However, as the hydrodynamic properties of a protein may be significantly modified in the presence of detergent, we looked for other evidence to confirm the trimeric nature of the native rabies virus glycoprotein.

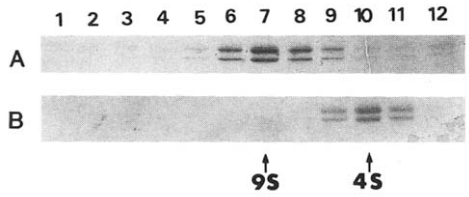

FIG. 2. Sedimentation profile of G protein in sucrose density gradients (see Material and Methods). (A) G was solubilized with 1% CHAPS. The sucrose gradient (in TD) also contained 1% CHAPS. (B) G was solubilized with 0.5% TRITON × 100. The sucrose gradient (in TD) contained also 0.5% TRITON × 100. Gradients were fractionated from the bottom and each fraction was analyzed by SDS–PAGE.

The oligomeric structure of G also appeared to be crucially dependent on the CHAPS concentration: increasing the concentration to 2% (32.4 m*M*) rendered G monomeric while decreasing the CHAPS concentration to 0.5% (8.1 mM) led to self-aggregation of G. Therefore, the purification protocol described under Materials and Methods was routinely used for further experiments.

Morphology of G protein on virus

When rabies virus (50L1) was prepared for electron microscopy by negative staining with SST, which has a natural pH of 7, G could be seen in side view on the periphery of the virions and in end-on view on the surface of the virus particles (Fig. 3). The virus particles were deformed during the preparation procedure which helped visualization of G as it spread out the proteins so that individual complexes could be seen. Seen in side view, G looked like a head on a thin stalk, resembling the influenza neuraminidase (Ruigrok *et al.*, 1986). The total length of the spike was 8.3 nm (for standard deviations and number of measurements, see Fig. 6). The height of the head was about 4.8 nm which left 3.5 nm for the stalk. Even when the stalk was not visible in Fig. 3, we assumed that the amount of G protein mass near the membrane was less than that at the position of the head since there was stain accumulation between head and membrane.

In end-on view, triangles consisting of three dots were frequently observed in the regions where there were only few molecules. The side of the triangle measured 8.4 nm. This indicated that, on the virus, G had a trimeric quaternary structure. When the density of G on the viral surface was too high, separated triangles were not recognized.

Morphology of detergent-isolated G protein

When detergent-isolated G was negatively stained with SST, different two-dimensional projections of the various aggregation states of an asymetric structure could be observed (Fig. 4A). Upon close examination, we could discern three major types of shape labeled B, C, and D in Fig. 4A, that are shown with higher magnifi-

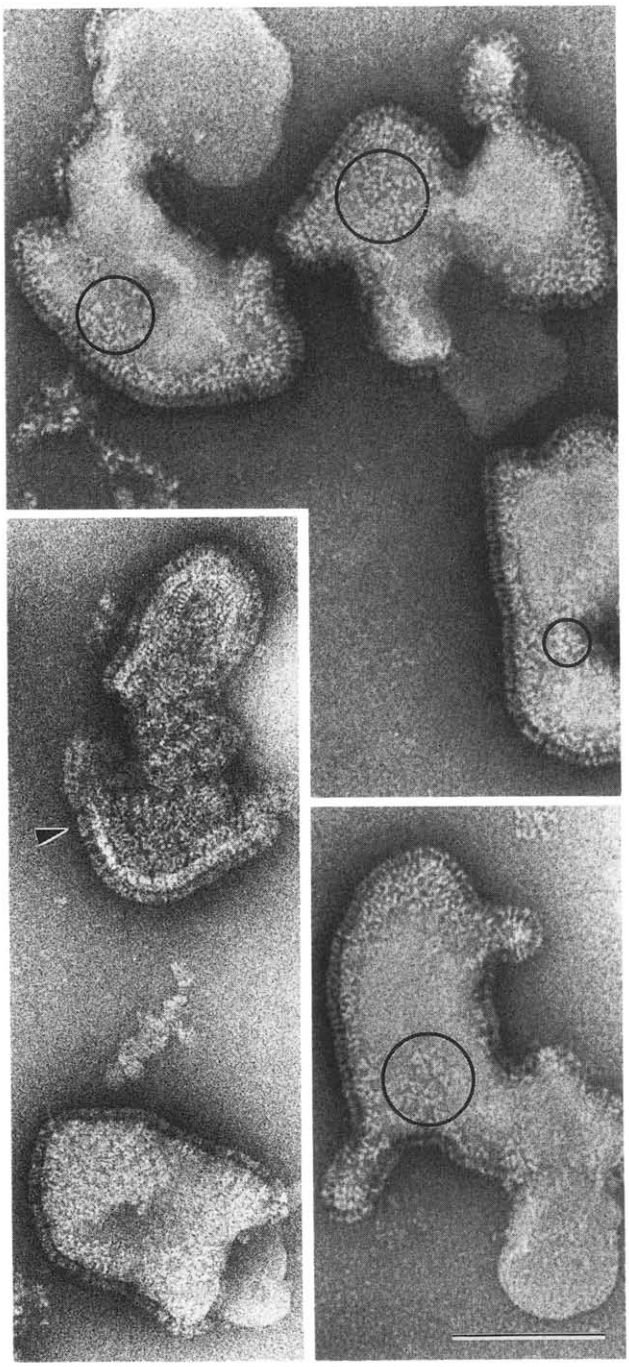

FIG. 3. Composition of electron micrographs of negatively stained rabies virus. The G protein spikes can be seen in side view in the periphery of the virus and in end-on view showing the trimeric nature of the spikes. The arrowhead points to a region where the heads of the spikes in side view are resolved into two dots and where the stalk is visible. Regions where triangles are clearly visible are encircled. The bar represents 100 nm.

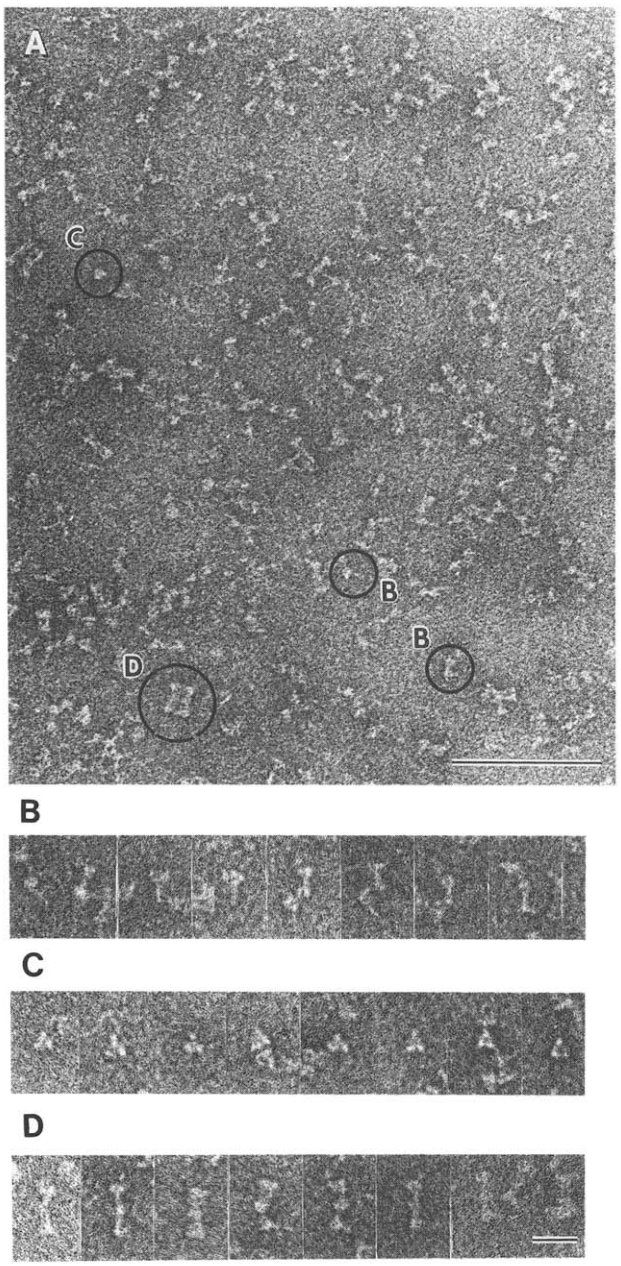

FIG. 4. (A) Electron micrograph of negatively stained detergent-isolated G. The molecules encircled in (A) are shown with a higher magnification in the galleries B–D. (B) Side view of a single G molecule. (C) Trimeric end-on view of a single G molecule. (D) Doublet of trimers associated via their hydrophobic transmembrane ends. The molecule D encircled in (A) shows two of these doublets lying side-by-side. The bar in (A) represents 100 nm and the bar in (D) which indicates the magnification for all three galleries, represents 20 nm.

cation in the corresponding galleries of Figs. 4B, 4C, and 4D.

Figure 4B shows a side view of isolated spikes; a head on a stalk with a total length of 13.2 nm, the head being 6.1-nm wide and 5.0-nm high. Isolated spikes were 4.9 nm longer than spikes extending from the membrane of virus, which was consistent with the additional presence of the transmembrane (residues 440–461) plus cytoplasmic parts (462–505) of G. About 25% of the spikes measured (the criterium for selection being a stalk with a head) were longer than 13.2 nm and showed a separate peak in the length distribution of 16.1 ± 0.4 nm (n = 34) (see Fig. 5). This higher value might be caused by a different orientation on the grid of one or both extreme ends of the molecule, or by different conformations of the molecule. Different orientations of the amino terminus of the adenovirus fiber protein also resulted in different overall lengths (Ruigrok *et al.,* 1990). Figure 4C shows the spike in end-on view, similar triangles as shown for the end-on view of G on virus, indicating clearly the trimeric nature of the spike formed by G. The side of the triangle measured 8.8 nm which was more than the average width of the head (6.1 nm) when seen in side view. The monomers making up the trimer seemed to have come somewhat apart when G was adsorbed head-on on the carbon film. Figure 4D shows doublets of trimers that are associated via their hydrophobic transmembrane parts. The total length of a doublet was 21.6 nm which agreed with twice the length of detergent-isolated G minus one transmembrane plus cytoplasmic part (13.2 + 13.2 − 4.9). The length of these doublet was well defined and the length distribution showed only one peak. This suggested that the single trimers with the length of 16.1 nm had a length extension at their N-terminal end when compared with the 13.2-nm spikes. Possibly, the cytoplasmic part of G of the 16.1-nm spike is folded differently, or is lying on the carbon film in a different manner than that of the 13.2-nm spike. Model drawings of G on virus, detergent-isolated single trimers, and doublets are shown in Fig. 6.

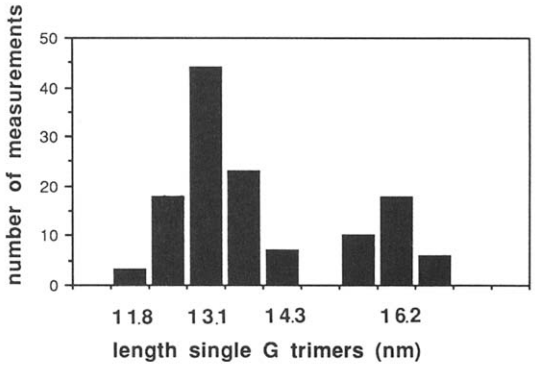

FIG. 5. Length distribution of single trimers of G. Note the separate distributions of the two populations, around 13.1 and 16.2 nm. The size classes, about 0.6-nm wide, are derived directly from the measurements from EM prints and, therefore, relate to the magnification of the prints (160.5K so 0.1 mm on the print corresponds to 0.62 nm).

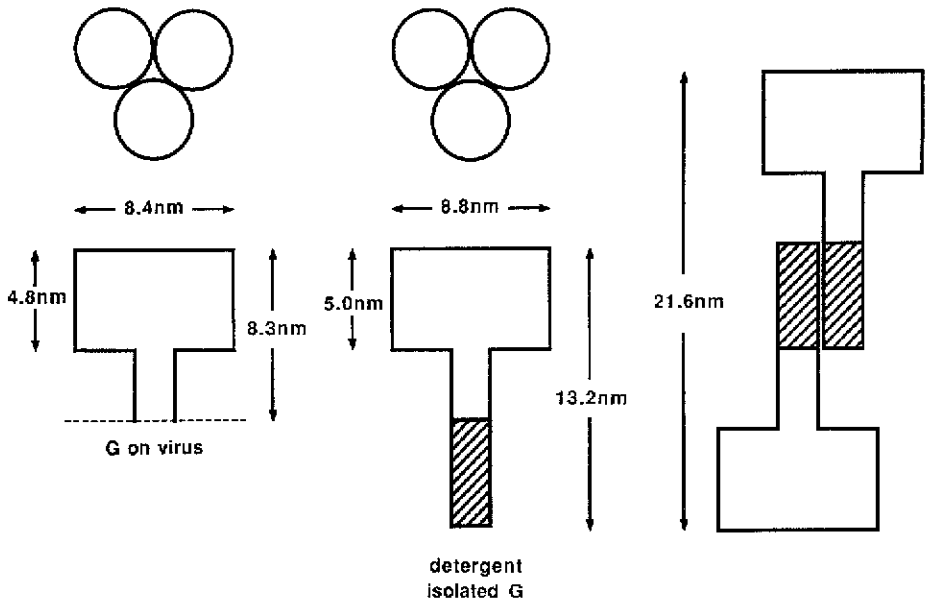

FIG. 6. Drawings of G on virus and detergent-isolated G, single trimers, and doublets. The dimensions are indicated but note that for the width of the heads we used the measurement of the sides of the triangles of the end-on orientation of G on the carbon film, which differs from the direct measurement of the width (see text). The transmembrane plus cytoplasmic parts of detergent-isolated G are shaded. In the drawing of the single trimer of detergent-isolated G, we have not taken into account the fraction of molecules that had a length of about 16 nm. The length of spikes extending from the viral membrane was 8.3 ± 0.5 nm (number of measurements: $n = 80$); the height of the head of viral G was 4.8 ± 0.7 nm ($n = 22$), the side length of the triangles observed on virus was 8.4 ± 1.1 nm ($n = 41$), the length of detergent-isolated spikes was 13.2 ± 0.6 nm ($n = 95$), and the height and the width of their head were, respectively, 5.0 ± 1.0 nm ($n = 43$) and 6.1 ± 0.9 nm ($n = 47$), whereas the side length of isolated triangles was 8.8 ± 0.6 nm ($n = 93$). The length of doublets was 21.6 ± 1.0 nm ($n = 88$).

Apart from single trimers and doublets, many different aggregated forms of G may be observed in Fig. 4A. This aggregation was caused by dilution with PBS necessary for EM preparation. The same preparation diluted with PBS plus 1% CHAPS showed mainly separate, nonaggregated molecules of G (data not shown).

DISCUSSION

In this paper, we have investigated the quaternary structure of the glycoprotein G of rabies virus using electron microscopy of negatively stained samples. This technique allows reliable results and measurements (Ruigrok *et al.*, 1986) provided that the protein is not denatured by the preparation procedure. When we measured the length of G via cryoelectron microscopy of frozen hydrated virus which is supposed to be a nondenaturing technique, we obtained a similar result as presented here from negatively stained virus (Hewat and Ruigrok, unpublished) suggesting that the staining procedure did not denature G.

First, our work has demonstrated that the rabies glycoprotein is organized as a trimer at the viral surface confirming the results obtained by Whitt *et al.* (1991) using a cross-linking reagent on G expressed in Hela cells from cloned cDNA. This trimer can be solubilized under its native quaternary structure with CHAPS, a zwitterionic detergent. However, once the glycoprotein is solubilized, this trimeric organization is not very stable and appears to be sensitive to most of the detergents that we used. Such an instability has also been reported in the case of VSV: solubilized with OG, VSV G appeared to be monomeric (Crimmins *et al.*, 1983) while, solubilized with Triton X100 at acidic pH, VSV G appeared to be trimeric (Doms *et al.*, 1987). Such a stabilization of the oligomeric structure at acidic pH was not observed in the case of rabies virus G (Whitt *et al.*, 1991; this work). Apparently, the oligomeric organization of the rhabdovirus glycoproteins is less stable than that of influenza virus hemagglutinin of which the trimeric organization is resistant to most detergents such as Triton X100 (Skehel *et al.*, 1982), Brij 36T (Skehel *et al.*, 1982; Ruigrok *et al.*, 1986), OG (Ruigrok *et al.*, 1986), and $C_{12}E_8$ (Stegmann *et al.*, 1987). This relative instability may also explain why the trimeric end-on view of detergent-isolated G and G on deformed virus shows a larger width (8.8 and 8.4 nm, respectively) for the head than detergent-isolated G in side view (6.1 nm).

Numerous viral external proteins such as the adenovirus fiber (Ruigrok *et al.*, 1990), the reovirus cell attachment protein 1 (Strong *et al.*, 1991), the corona-

virus spike protein (Delmas and Laude, 1990), the rhabdovirus glycoproteins (Doms *et al.,* 1987; this work), and the hemagglutinin of influenza virus (Wilson *et al.,* 1981), which are implicated in receptor recognition and/or carry the membrane fusion properties of the virion, are trimeric. This might have some biological significance and may reflect similarities in the mechanisms involved in receptor recognition and/or membrane fusion.

Electron microscopy also indicates that the native molecule has a "head" and a "stalk" and indications on the respective dimensions of those two parts have been obtained. The fact that rabies virus glycoprotein has a stalk may indicate that a certain flexibility of the head of the glycoprotein is required.

So far, very little is known about the structure of rabies virus glycoprotein. The glycoprotein isolated with CHAPS as described here will hopefully allow more detailed structural and biochemical studies.

ACKNOWLEDGMENTS

We thank J. Benejean and I. Sassoon for helpful technical assistance. Y. Gaudin is a predoctoral fellow from the Ecole Polytechnique. This work was supported by CNRS (UPR 2431).

REFERENCES

ANILIONIS, A., WUNNER, W. H., and CURTIS, P. J. (1981). Structure of the glycoprotein gene in rabies virus. *Nature (London)* **294,** 275–278.

ARITA, M., and ATANASIU, P. (1980). Etude comparative du poids moléculaire de plusieurs souches de virus rabique par électrophorèse sur gel de polyacrylamide. *Ann. Virol. (Inst. Pasteur)* **131E,** 201–215.

BRAND, C. M., and SKEHEL, J. J. (1972). Crystalline antigen from the influenza virus envelope. *Nature New Biol.* **230,** 145–147.

COULON, P., DERBIN, C., KUCERA, P., LAFAY, F., PRÉHAUD, C., and FLAMAND, A. (1989). Invasion of the peripheral nervous systems of adult mice by the CVS strain of rabies virus and its avirulent derivative Av01. *J. Virol.* **63,** 3550–3554.

CRIMMINS, D. L., MEHARD, W. B., and SCHLESINGER, S. (1983). Physical properties of a soluble form of the glycoprotein of vesicular stomatitis virus at neutral and acidic pH. *Biochemistry* **22,** 5790–5796.

DELAGNEAU, J. F., PERRIN, P., and ATANASIU, P. (1981). Structure of the rabies virus: spatial relationships of the proteins G, M1, M2 and N. *Ann. Virol. (Inst. Pasteur)* **132E,** 473–493.

DELMAS, B., and LAUDE, H. (1990). Assembly of coronavirus spike protein into trimers and its role in epitope formation. *J. Virol.* **64,** 5367–5375.

DIETZSCHOLD, B. (1977). Oligosaccharides of the glycoprotein of rabies virus. *J. Virol.* **23,** 286–293.

DIETZSCHOLD, B., COX, J. H., and SCHNEIDER, L. G. (1979). Rabies virus strains: A comparison study by polypeptide analysis of vaccine strains with different pathogenic patterns. *Virology* **98,** 63–75.

DIETZSCHOLD, B., COX, J. H., SCHNEIDER, L. G., WIKTOR, T. J., and KOPROWSKI, H. (1978). Isolation and purification of a polymeric form of the glycoprotein of rabies virus. *J. Gen. Virol.* **40,** 131–139.

DOMS, R. W., KELLER, D. S., HELENIUS, A., and BALCH, W. E. (1987). Role for adenosine triphosphate in regulating the assembly and transport of vesicular stomatitis virus G protein trimers. *J. Cell Biol.* **105,** 1957–1969.

GAUDIN, Y., TUFFEREAU, C., SEGRETAIN, D., KNOSSOW, M., and FLAMAND, A. (1991a). Reversible conformational changes and fusion activity of rabies virus glycoprotein. *J. Virol.* **65,** 4853–4859.

GAUDIN, Y., TUFFEREAU, C., BENMANSOUR, A., and FLAMAND, A. (1991b). Fatty-acylation of rabies virus proteins. *Virology* **184,** 441–444.

KUCERA, P., DOLIVO, M., COULON, P., and FLAMAND, A. (1985). Pathways of the early propagation of virulent and avirulent rabies virus strains from the eye to the brain. *J. Virol.* **55,** 158–162.

LAEMMLI, U. K. (1970). Cleavage of structural proteins during the assembly of the head of bacteriophage T4. *Nature (London)* **227,** 680–685.

LAFAY, F., COULON, P., ASTIC, L., SAUCIER, D., RICHE, D., HOLLEY, A., and FLAMAND, A. (1991). Spread of the CVS Strain of rabies virus and of the avirulent mutant Av01 along the olfactory pathways of the mouse after intranasal inoculation. *Virology* **183,** 320–330.

MIFUNE, K., OHUCHI, M., and MANNEN, K. (1982). Hemolysis and cell fusion by rhabdoviruses. *FEBS Lett.* **137,** 293–297.

RUIGROK, R. W. H., WRIGLEY, N. G., CALDER, L. J., CUSACK, S., WHARTON, S. A., BROWN, E. B., and SKEHEL, J. J. (1986). Electron microscopy of the low pH structure of influenza virus haemagglutinin. *EMBO J.* **5,** 41–49.

RUIGROK, R. W. H., BARGE, A., ALBIGES-RIZO, C., and DAYAN, S. (1990). Structure of adenovirus fibre. II. Morphology of single fibres. *J. Mol. Biol.* **215,** 589–596.

SKEHEL, J. J., BAILEY, P. M., BROWN, E. B., MARTIN, S. R., WATERFIELD, M. D., WHITE, J. M., WILSON, I. A., and WILEY, D. C. (1982). Changes in the conformation of influenza virus hemagglutinin at the pH optimum of virus-mediated membrane fusion. *Proc. Natl. Acad. Sci. USA* **79,** 968–972.

STEGMANN, T., MORSELT, H. W. M., BOOY, F. P., VAN BREMEN J. F. L., SCHERPHOF, G., and WILSHUT, J. (1987). Functional reconstitution of influenza virus envelopes. *EMBO J.* **6,** 2651–2659.

STRONG, J. E., LEONE, G., DUNCAN, R., SHARMA, R. K., and LEE, P. W. K. (1991). Biochemical and biophysical characterization of the reovirus cell attachment protein 1: evidence that it is a homotrimer. *Virology* **184,** 23–32.

WHITT, M. A., BUONOCORE, L., PRÉHAUD, C., and ROSE, J. K. (1991). Membrane fusion activity, oligomerization, and assembly of the rabies virus glycoprotein. *Virology* **185,** 681–688.

WIKTOR, T. J., GYÖRGY, E., SCHLUMBERGER, H. D., SOKOL, F., and KOPROWSKI, H. (1973). Antigenic properties of rabies virus components. *J. Immunol.* **110,** 269–276.

WILSON, I. A., SKEHEL, J. J., and WILEY, D. C. (1981). Structure of the hemagglutination membrane glycoprotein of influenza virus at 3A resolution. *Nature (London)* **289,** 368–373.

WUNNER, W. H., REAGAN, K. J., and KOPROWSKI, H. (1984). Characterization of saturable binding sites for rabies virus. *J. Virol.* **50,** 691–697.

WUNNER, W. H., DIETZSCHOLD, B., SMITH, C. L., LAFON, M., and GOLUB, E. (1985). Antigenic variants of CVS rabies virus with altered glycosylation sites. *Virology* **140,** 1–12.

YELVERTON, E., NORTON, S., OBIJESKI, J. F., and GOEDDEL, D. V. (1983). Rabies virus glycoprotein analogs: biosynthesis in Escherichia coli. *Science* **219,** 614–620.